

# Pluggable Sockets for Point-of-Load Converters in Distributed Power Systems

Phillip Henson<sup>1</sup>, Josh Connell<sup>1</sup>, R. Wayne Johnson<sup>1</sup>, Mark Nelms<sup>1</sup>, Prashant Joshi<sup>2</sup>, Bill Miller<sup>2</sup> and John Comish<sup>3</sup>

<sup>1</sup>Auburn University, <sup>2</sup>Interconnect Systems, Inc, <sup>3</sup>Department of Defense

<sup>1</sup>200 Broun Hall, ECE Dept. Auburn, AL 36849

<sup>2</sup>759 Flynn Road, Camarillo, CA 93012

johnson@eng.auburn.edu

Prashant.Joshi@isipkg.com

john.w.comish@ugov.gov

## Abstract

A pluggable surface mount socket has been developed for use in mounting point-of-load dc-dc converters. The socket has high current (40A) capability and low electrical resistance (ave = 0.67mΩ). The resistance is stable with multiple mating cycles, humidity storage and thermal shock cycling. The socket does not introduce additional length to the thermal path for heat removal to the motherboard. In the current application, heat is removed from the top of the dc-dc converter as well as through the socket and motherboard.

## Introduction

With high performance microprocessors and application specific integrated circuits (ASICs) requiring high current at low voltage levels, distributed, point-of-load power supplies are required. High density, 1/4 and 1/8 brick dc-dc converters are often used in telecom and other applications [1, 2]. While these bricks are commercially available in a surface mount assembly configuration, their thermal mass creates challenges in achieving an acceptable reflow profile when many bricks are assembled on a thick motherboard along with a variety of other components with significantly lower thermal masses. For products that are expected to operate for 10-20 years, the ability to remove and replace power supplies in the field is also a lifecycle support consideration. It is a challenge to supply sufficient heat with a soldering iron to a large copper lead soldered to thick copper power or ground planes in the motherboard without damaging the motherboard. Hot air rework faces a similar challenge with heat sinking from the motherboard and the power supply leads. To address these issues, a surface mountable socket has been designed and fabricated. The socket has low thermal mass and can be reflow soldered onto the motherboard. The pinned dc-dc converter is then simply plugged into the socket. This configuration reduces repair time from several minutes to a few seconds and clearly addresses the need for field repair.

## Socket Design

The socketed power supply design had to address multiple simultaneous requirements. It had to be easy to insert and extract the dc-dc converter, preferably without any tooling. The power pins and socket contacts had to have a current carrying capacity of 40A with minimal voltage drop. Also, it had to withstand high clamping forces from cold plates used in the final application. All of the above requirements were met by over-molding a lead frame with screw machined receptacles soldered to it, (Figure 1).

To meet the force requirements, an inner contact with relatively low insertion-extraction forces was used in the receptacle. The insertion force is approximately 150 gm per

contact while the extraction force is approximately 70 gm per contact. For an 8-pin dc-dc converter, this resulted in a hand insertable/extractable design. To satisfy current carrying capacity and voltage drop requirements, the receptacle shell was designed with the largest cross sectional area possible for the package. The shells were soldered to a copper lead frame to improve heat dissipation. The lead frame was Ni/Au plated for solderability. Since the power pins/contacts were required to carry 40A, an inner contact with a 6 finger design was selected. To minimize resistance, the pins were designed with high conductivity tellurium copper and with the largest diameter the contact would accept. Pin and shell geometries were designed to the lowest profile possible to maximize heat dissipation from the contact interface into the printed circuit board and cold plate and to minimize the overall height profile. Since the cold plate used in this application has high clamping forces, the lead frame leads were designed with a gull wing to provide compliancy. The over-molded housings had stand-offs to prevent overstressing of the solder joints when under the compressive load of the cold plate. (Figures 1 & 2). The leads extend 25-50µm below the molded stand-offs. Support features (Figure 1) were also molded into the plastic housing to support the underside of the dc-dc converter when the cold plate clamping forces were applied to the top surface of the converter.

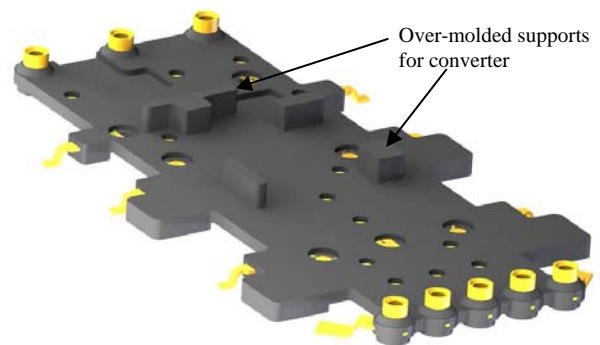


Figure 1. Pluggable Power Supply Socket

Selection of the over molding polymer was based on molding characteristics, dimensional stability, flatness and coplanarity as-molded and flatness and coplanarity after exposure to a reflow cycle. Flatness refers to the flatness of the molded plastic body, while coplanarity refers to the coplanarity of the 8 leads. To ensure molded parts stayed flat during reflow, proper resin selection was important. Based on supplier data sheets, two resins were selected. A different

connector design was molded with both resins and assembled connectors were subjected to a eutectic tin/lead reflow profile. Flatness and coplanarity values, before and after reflow, for the tested parts are shown in Figures 3 and 4. Resin from supplier B showed flatter parts before and after reflow and hence was selected for further analysis. Power supply sockets were then molded with the selected resin. Figures 5 and 6 plot the flatness and lead coplanarity initially and after a reflow cycle. The socket was placed on a printed circuit board without solder paste and subjected to the eutectic Sn/Pb solder reflow profile. Both flatness and coplanarity were well within the design specification of 0.005" (127 $\mu$ m). Figures 7 and 8 show histograms of flatness and lead coplanarity measurements from production sockets.

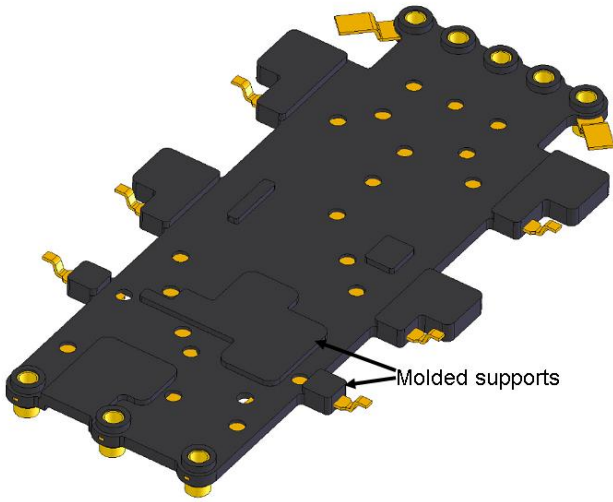


Figure 2. Underside of Socket Showing Molded Supports

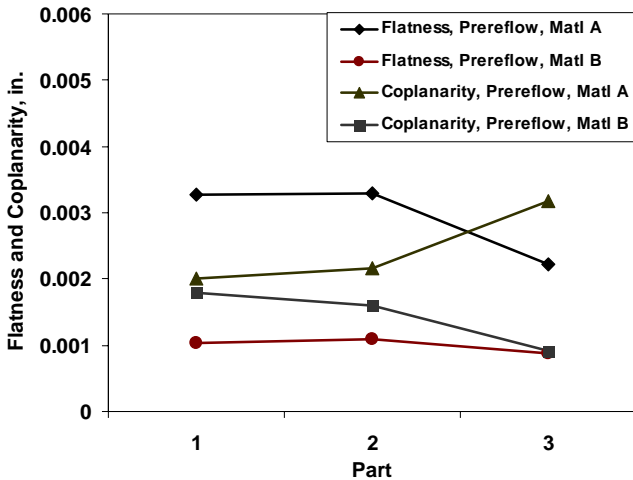


Figure 3. Material Comparison for Flatness and Coplanarity Prior to Reflow

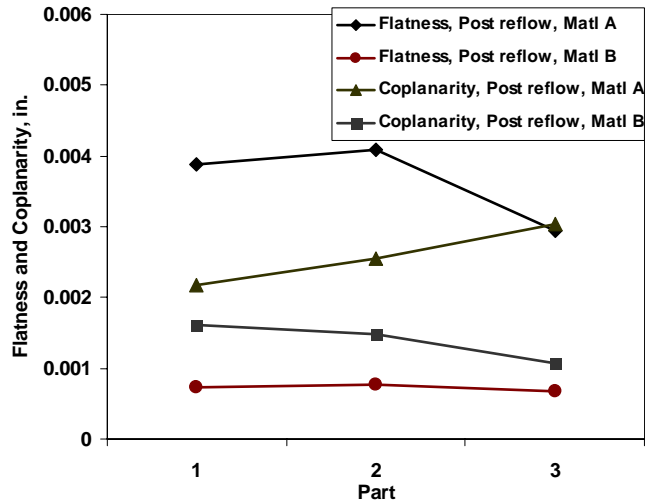


Figure 4. Material Comparison for Flatness and Coplanarity After Reflow

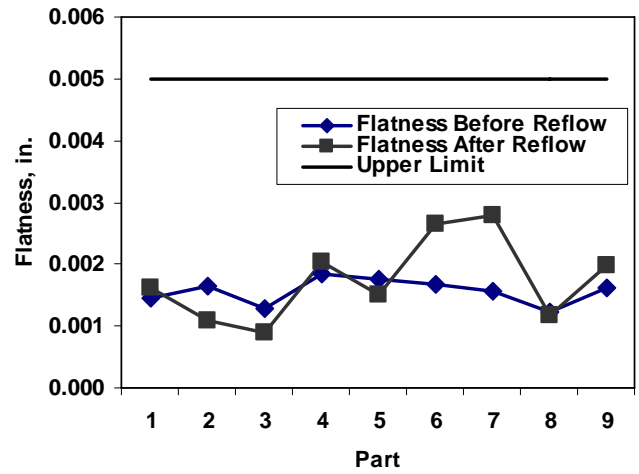


Figure 5. As-molded and After Reflow Socket Flatness

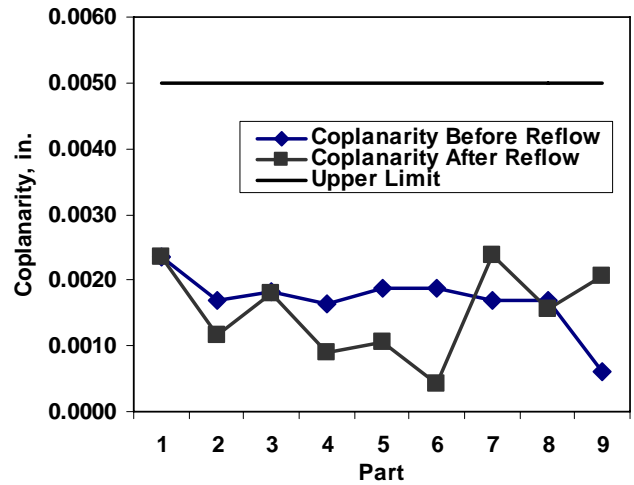


Figure 6. As-molded and After Reflow Lead Coplanarity

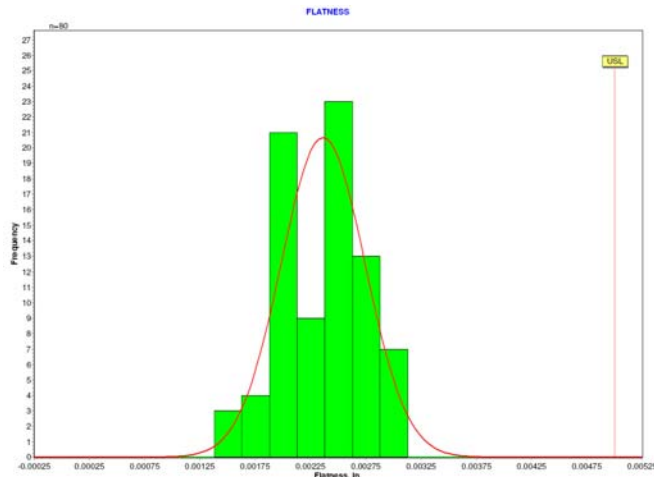


Figure 7. Flatness Measurements from Production Sockets

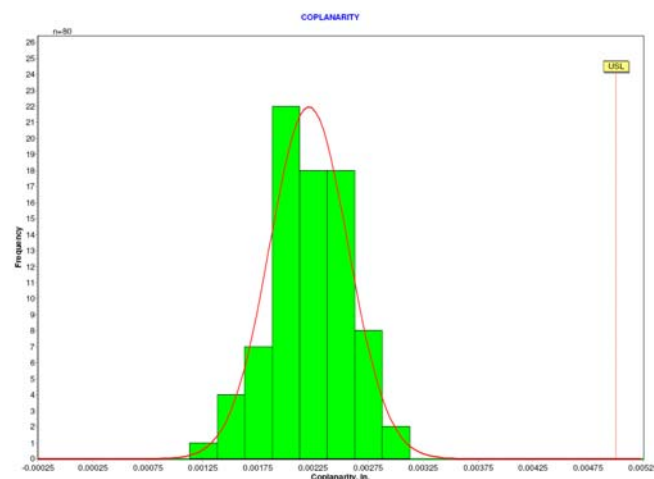


Figure 8. Lead Coplanarity Measurements from Production Sockets

For low contact resistance, the contact fingers were Ni/Au plated with a minimum Au specification of  $25\mu\text{in}$  ( $0.635\mu\text{m}$ ) and a target of  $30\mu\text{in}$  ( $0.76\mu\text{m}$ ). Figure 9 plots production Au thickness measurements. The lead frame was also Ni/Au plated for solderability during board level assembly. As shown in Figure 10, the Au thickness is biased toward the lower limit to avoid Au embrittlement of the solder joint.

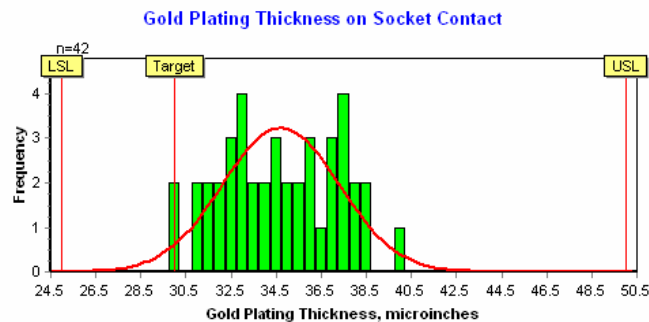


Figure 9. Au Plating Thickness on the Socket

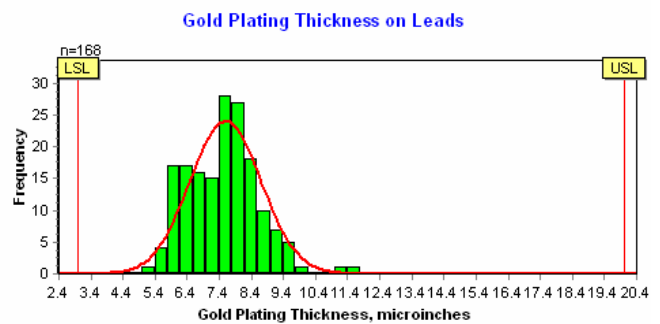


Figure 10. Lead Frame Au Thickness

### Assembly

The socket is shipped in a custom JEDEC tray that protects the leads and is compatible with standard pick and place equipment. No special nozzles are required for placement. Sockets have been successfully assembled in volume production using a conventional tin/lead solder paste and reflow profile. The lead co-planarity achieved with the socket has resulted in a very high assembly yield, meeting IPC J-STD-001, Class 3 solder joint requirements. Figure 11 shows a socket soldered to the production board. In Figure 12, the dc-dc converter has been plugged into the socket.

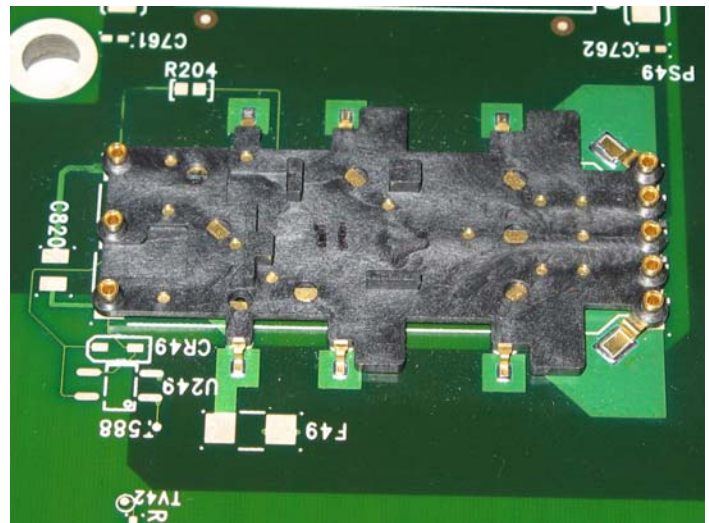


Figure 11. Socket Soldered to Production Board

Test vehicles have been assembled at Auburn University to evaluate the assembly process and the electrical and thermal performance of the socket. A  $150\mu\text{m}$  thick stencil was used to print the Kester EasyProfile 126 Sn/Pb eutectic solder paste. The apertures for the two large, high current pads were designed equal to the solder mask opening, while the apertures for the six smaller pads were designed 25% larger than the solder mask opening. While solder ball formation due to solder paste overprint on the solder mask was not observed, the solder mask opening could be increased to avoid overprinting. As shown in Figure 13, the pads on the test board were solder mask defined. For high current and thermal performance, large copper pads are used and the

solder mask opening could easily be increased. Solder mask defined pads are also used on the production board.

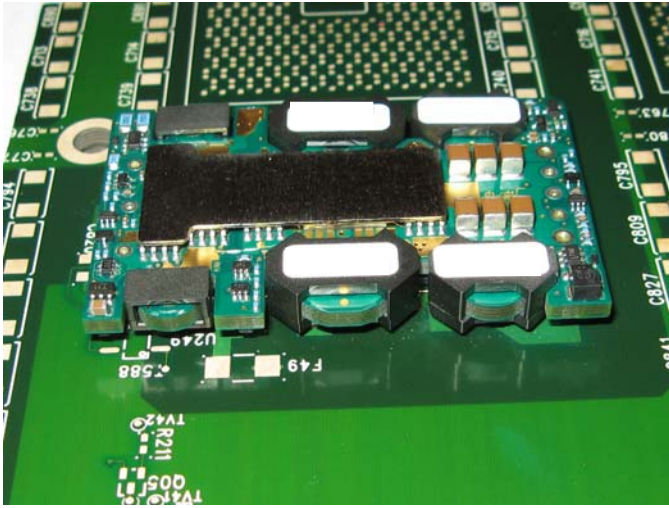


Figure 12. dc-dc Converter Plugged into Socket

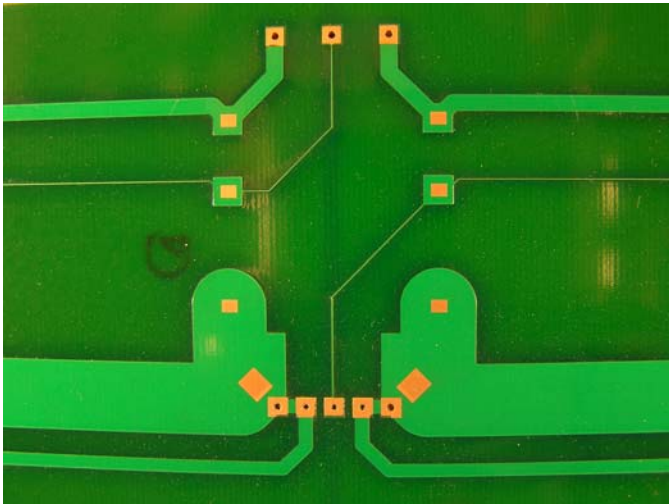


Figure 13. Photograph of Test Board Showing Solder Mask Defined Pads

The sockets were then placed and reflowed. The reflow profile is shown in Figure 14. The peak temperature for the output power pads was slightly lower due to the Cu area tied to those pads.

### Electrical Testing

The dc-dc converter used in this application had two sense lines that sense the voltage at the load and provide feedback to the converter. The output voltage of the converter is controlled to compensate for the resistive losses between the converter output pins and the load to maintain the proper voltage at the load at any current level. In the test vehicle design, the sense voltage was measured at the board surface near the socket power and ground leads. Thus the difference in the output voltage (as measured directly on the dc-dc converter) and the sense voltage (measured near the power

and ground socket leads on the test board) was equal to the voltage drop through the socket power and ground connections. Figure 15 plots typical output and sense voltages as a function of load current for a 1.8V dc-dc converter. A variable resistor was used for the load. The increase in output voltage with current is nearly linear. The decrease in sense voltage over the current range from 0 to 42.6A was only 3.08mV – very good load regulation.

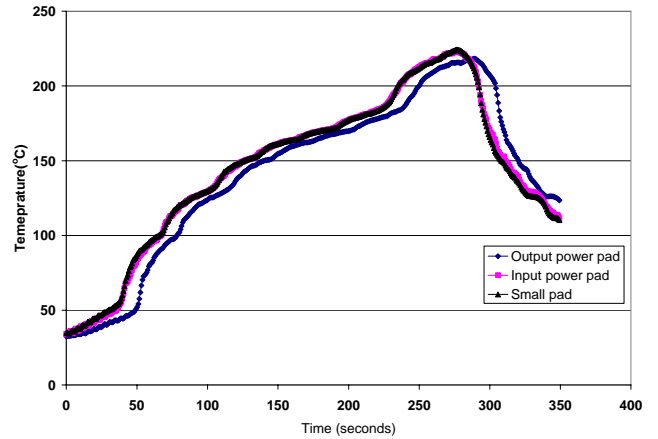


Figure 14. Reflow Profile for Assembly of Test Vehicle

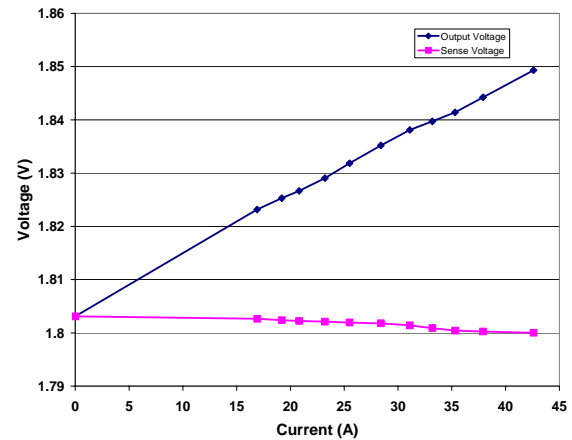


Figure 15. Typical  $V_{output}$  and  $V_{sense}$  as a Function of Load Current for a 1.8V dc-dc Converter

The resistance of the ground and power connections are of interest. The resistance associated with a pin and contact (pin, contact and lead frame) can be calculated as  $\frac{1}{2} (V_{output} - V_{sense}) / I_{load}$ . The factor of  $\frac{1}{2}$  is used since the measurement includes two pins (power and ground). Figure 16 plots typical  $\frac{1}{2} (V_{output} - V_{sense})$  versus  $I_{load}$  for 1.8V converters. Figure 17 plots the calculated pin and contact resistance at a 30A load current for forty 1.3V dc-dc converters. The mean resistance is 0.67m $\Omega$  and the standard deviation is 0.067 m $\Omega$ .

The repeatability of the voltages and resistance with multiple plug and unplug cycles was measured. A typical plot of  $V_{output}$  and  $V_{sense}$  as a function of mating cycles is plotted in Figure 18. The load current was 40A. The results are very consistent with mating cycles.

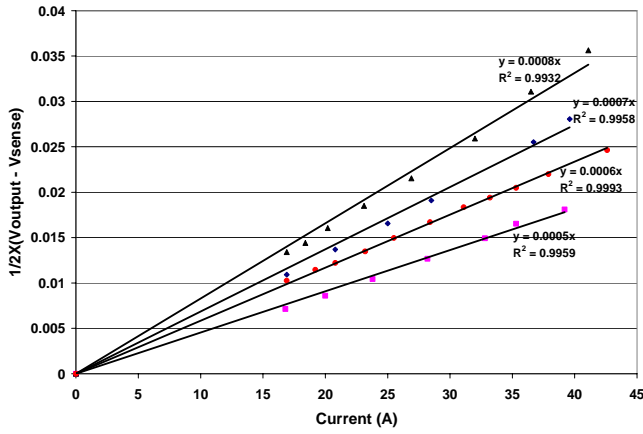


Figure 16.  $\frac{1}{2}(V_{\text{output}} - V_{\text{sense}})$  as a Function of Load Current. The slope of each line is the resistance for a pin and contact

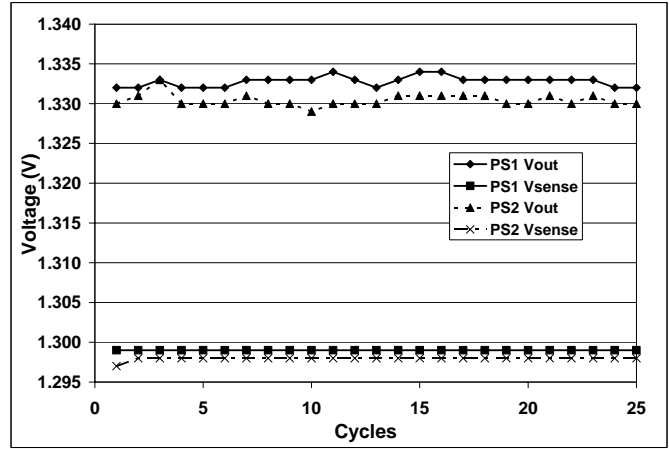


Figure 18.  $V_{\text{output}}$  and  $V_{\text{sense}}$  as a Function of Mating Cycles

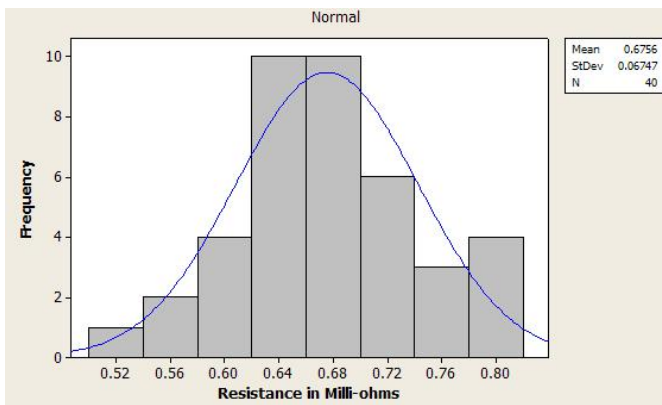


Figure 17. Histogram of Calculated Resistance for a Pin and Contact. The dc-dc converter nominal output was 1.3V and the load current was 30A into a resistive load.

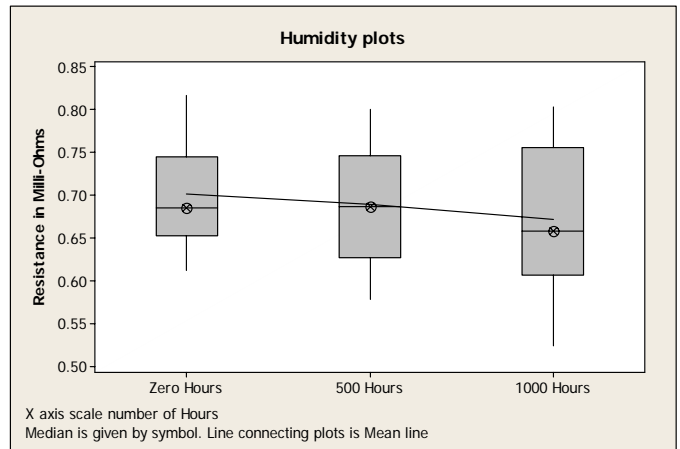


Figure 19. Calculated Resistance as a Function of Storage Time at 85°C/85%RH

Mated assemblies (20 samples) were subjected to unpowered storage at 85°C/85%RH. Figure 19 plots the calculated pin and contact resistance initially and after 500 and 1000 hours of storage. The voltages were measured and the resistance calculated at a load current of ~30A. 1.3V dc-dc converters were used. There was no significant change in mean resistance with temperature/humidity storage.

Air-to-air thermal shock testing was also performed on mated assemblies (20 samples). A two chamber system was used. The temperature extremes were -40°C and 125°C. The temperature profile measured on an assembly in the chamber is shown in Figure 20. 1.3V dc-dc converters were used. The voltages were measured and the resistance calculated with a load current of ~30A. The results are plotted in Figure 21. After 1000 thermal shock cycles the mean resistance was approximately the same as the initial mean. An increased mean resistance (~10%) was measured after 500 cycles. The cause of this small increase is not known.

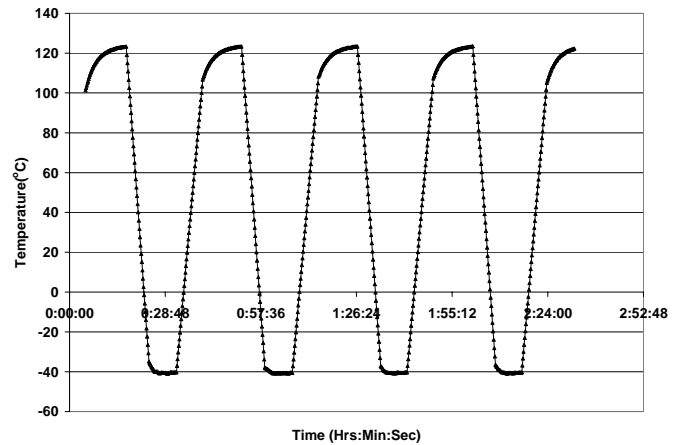


Figure 20. Measured Thermal Shock Profile

### Thermal Performance

The dc-dc converter is designed with thick internal copper planes that conduct heat to the pins. Heat is transferred from the power FET's through the four drain leads of the SOIC-8 packages to large copper pads and internal planes in the converter board. The converter was originally designed for the

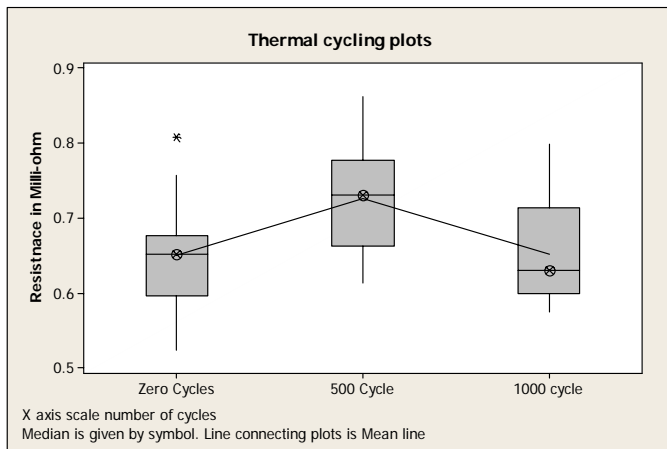


Figure 21. Calculated Resistance as a Function of Thermal Shock Cycles

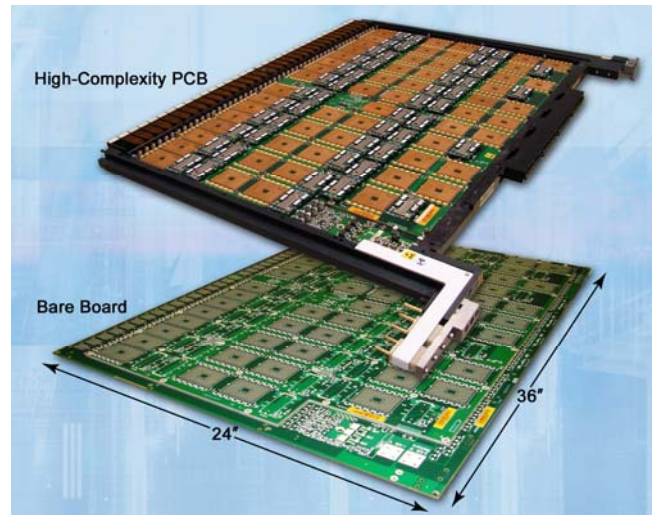


Figure 22. Assembled Production Motherboard (Courtesy: Endicott Interconnect)

eight I/O pins on the converter to be wave soldered into a motherboard. An alternate version of the converter is surface mountable with large leads that solder to the surface of the motherboard. In both cases, the thermal management scheme is to conduct the heat from the converter through the pins/leads to the motherboard where it is spread and dissipated through thick copper layers in the motherboard. In the application for which the socket was designed, an additional path for heat flow is through a thermal pad placed in contact with the top surface of the converter into the system cold plate. Figure 22 shows an assembled motherboard, while Figure 23 shows a corresponding cold plate with thermal pads. The final assembly with cold plate attached is shown in Figure 24. The cold plate has flowing Fluorinert® to extract the heat. Thus, heat is extracted both from the top surface of the converter and through the mother board.

For other applications, the impact of the socket on thermal performance must be considered. The test vehicle was instrumented with thermocouples as shown in Figures 25-27. In Figure 25 thermocouples were soldered to the pin connections for the Converter Ground Input (CGI), the Converter Power Output (CPO) and the Converter Circuit Board (CB) and attached to the top surfaces of two FET's (FET 1 and FET 8). The heat spreader shown in Figure 12 was removed for these tests. According to the dc-dc converter datasheet, the temperature measured at CB should not exceed 118°C in order to operate within the derating curves. In Figure 26, thermocouples were attached to the Socket Ground Input Lead (SGI) and the Socket Power Output Lead (SPO). In Figure 27, two thermocouples were attached to the backside of the test board (B1 and B2). The backside of the board had two large Cu planes (2oz Cu). One plane was tied to the Output Ground by a single plated through hole and the other plane was tied to the Output Voltage by a single plated through hole. The planes were covered with solder mask.

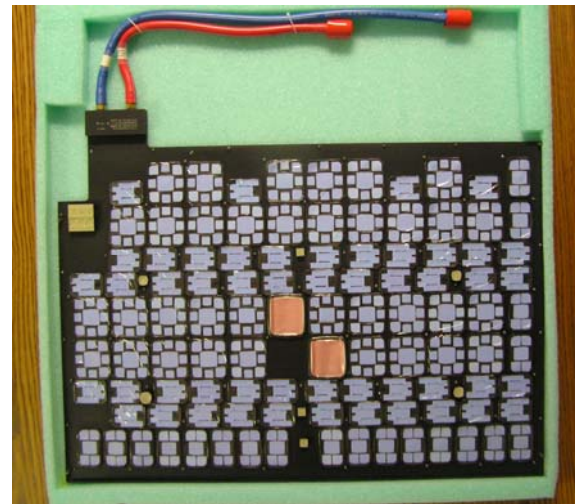


Figure 23. Cold Plate with Individual Thermal Pads Pre-attached for the dc-dc Converters and Other Components

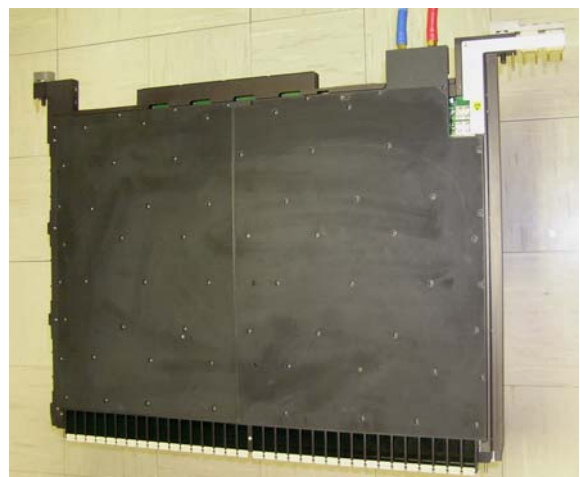


Figure 24. Final Assembly with Cold Plate Attached to Motherboard

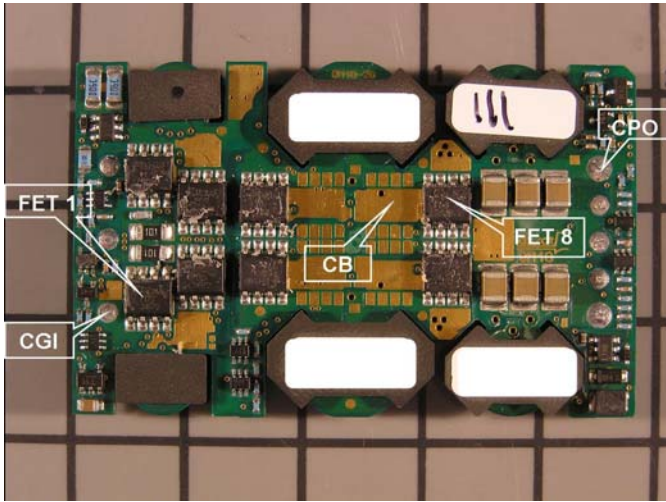


Figure 25. Thermocouple Locations on the dc-dc Converter

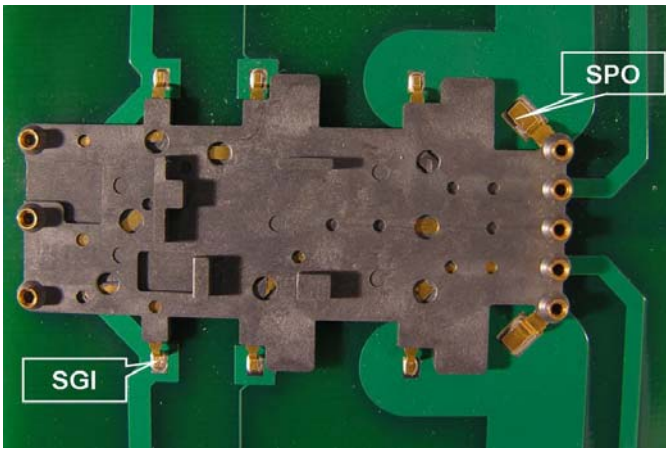


Figure 26. Thermocouple Locations on the Socket Leads

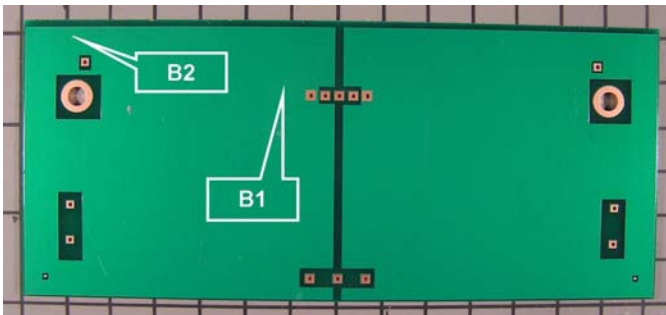


Figure 27. Thermocouple Locations on the Backside of the Test Board

A series of thermal measurements were made with the test board placed horizontal on insulating foam. In this configuration, the test board was not an effective heat sink. Figure 28 shows a typical temperature plot at a load current of 20.2A with a 1.3V dc-dc converter. The converter pins and the converter circuit board were nearly the same temperature. The tops of the FET packages were somewhat cooler than the converter board, corresponding to the primary heat path into the converter circuit board. The Socket Power Output (SPO)

and the Socket Ground Input (SGI) leads were nearly the same temperature and  $\sim 20^{\circ}\text{C}$  cooler than the corresponding pins on the converter (CPO and CGI). Temperatures B1 and B2 indicate the temperature gradient along the test board backside plane.

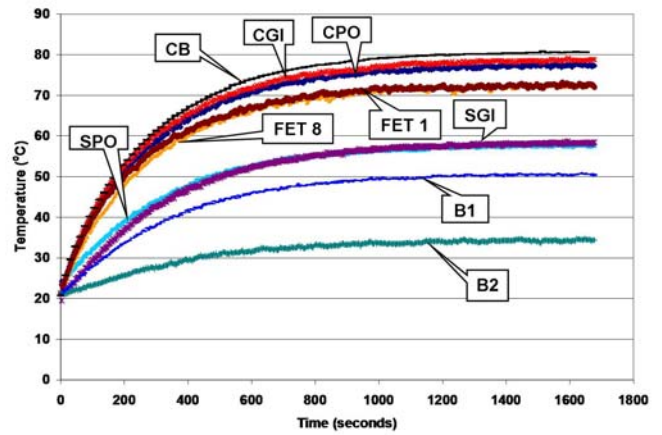


Figure 28. Temperature Profiles with the Test Board placed on an Insulating Foam. Current = 20.2A

Next a series of measurements were made with the board in a horizontal position, but this time with forced air blowing on the bottom of the board. The airflow was perpendicular to the bottom of the board. The board prevented any direct airflow on the converter. Figure 29 shows a typical temperature plot at a load current of 19.53A with a 1.3V dc-dc converter. In this configuration, the board was a better heat sink, B2 remained at room temperature and B1 was  $21^{\circ}\text{C}$  lower than in Figure 28. By cooling the backside of the board, the peak measured temperatures decreased by  $\sim 23^{\circ}\text{C}$ . Thus, with a motherboard designed to heat sink the converter through the socket, lower converter operating temperatures can be achieved.

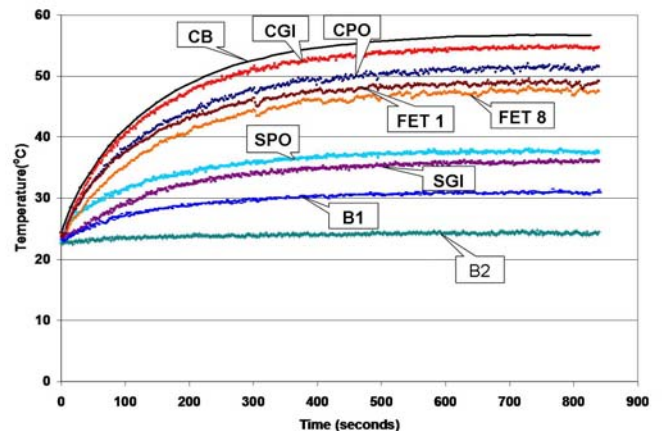


Figure 29. Temperature Profiles with Forced Air Blowing Perpendicular to the Bottom of the Test Board. Current = 19.53A

Figure 30 shows the thermal measurement results with the test board again placed on the insulating foam, but with air flowing across the top surface of the converter. The load

current was 20.27A from a 1.3V converter. The flow rate was 105fpm and the flow direction was from CPO (and FET 8) to CGI (and FET 1). The peak measured temperature was 53.6°C. The top package surface of FET 8 was cooler than FET 1 corresponding to the direction of airflow.

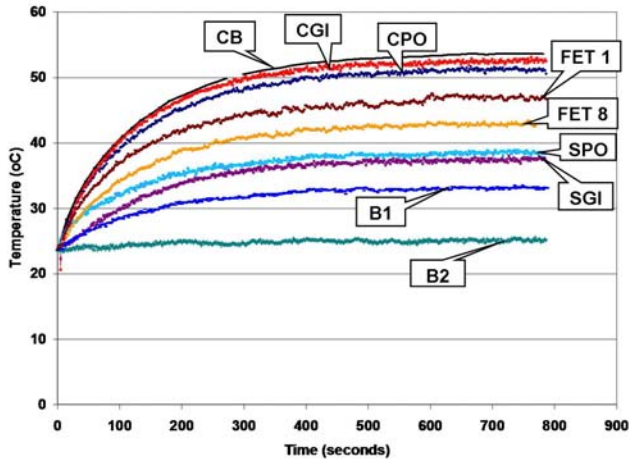


Figure 30. Temperature Profiles with Forced Air Blowing Across the dc-dc Converter. Current = 20.27A

Figure 31 plots the thermal measurements at 38.5A with a 1.3V dc-dc converter with airflow on the bottom of the test board (perpendicular flow). The peak measured temperature was 111.6°C at point CB, less than the manufacturer’s temperature limit. FET 8 and CPO and SPO are all higher than the corresponding FET 1, CGI and SGI since increasing the output current increases the power dissipation more in the output stages than in the input stages of the dc-dc converter.

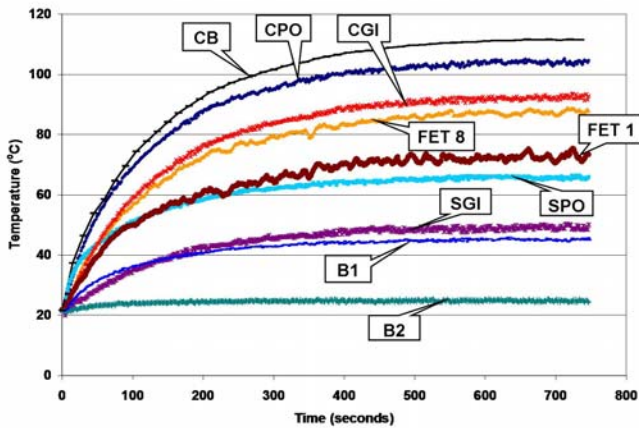


Figure 31. Temperature Profiles with Forced Air Blowing Perpendicular to the Bottom of the Test Board. Current =38.5A

A temperature profile for a 1.3V converter operating with a load current of 39.32A and airflow of 133fpm across the power supply is shown in Figure 32. The flow direction was from CPO (and FET 8) to CGI (and FET 1). The peak temperature was 107.8°C, only slightly cooler than with backside airflow on the test board.

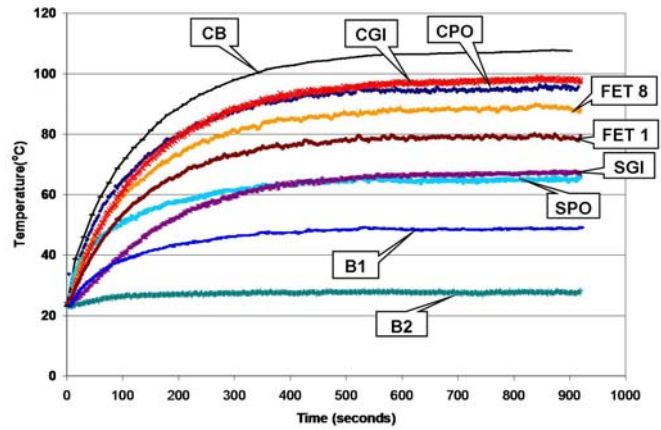


Figure 32. Temperature Profiles with Forced Air Blowing Across the dc-dc Converter. Current =39.32A

These thermal test results indicate that at full rated current (40A), the peak converter board temperature can be maintained below the limit by surface air flow or by heat sinking through the motherboard (direct air flow on the bottom of the test board in these experiments). The thermal performance with the socketed dc-dc converter will be a function of the system thermal design.

### Conclusions

An effective dc-dc converter mounting approach was developed that meets the potentially conflicting needs of ease of assembly, simple life cycle support, producibility in high volume production, thermal and electrical performance and long term reliability. While this application has unique heat management requirements this approach shows great promise in other point of load power delivery applications.

### Acknowledgments

The authors would like to acknowledge Endicott Interconnect for manufacturing of boards using the socket.

### References

1. White, Robert V., “Using On-Board Power Systems,” Proceedings of the 26th Annual International Telecommunications Energy Conference (INTELEC 2004), pp. 234-240.
2. White, Robert V., “Digital Power System Management,” Proceedings of the 20th Annual IEEE Applied Power Electronics Conference, March 2005, pp. 176-182.